Article

Sustainable CO$_2$ Refrigeration System for Fish Cold Storage Facility Using a Renewable Integrated System with Solar, Wind and Tidal Energy for Cape Verde—Analyzing Scenarios

João Garcia [1,2,3,*] and Arian Semedo [1,*]

1   Instituto Superior de Engenharia de Lisboa, Polytechnic University of Lisbon, R. Conselheiro Emídio Navarro 1, 1959-007 Lisboa, Portugal
2   The Unit for Innovation and Research in Engineering, Instituto Superior de Engenharia de Lisboa, Polytechnic University of Lisbon, R. Conselheiro Emídio Navarro 1, 1959-007 Lisboa, Portugal
3   Marine and Environmental Sciences Centre, Instituto Politécnico de Setúbal, 2910-761 Setúbal, Portugal
*   Correspondence: joao.garcia@isel.pt (J.G.); ariansemedo1997@hotmail.com (A.S.)

Abstract: This study compares four feasible alternative solutions for an integrated cold storage system in the city of Tarrafal, Santiago, Cape Verde. Integrated systems using grid electricity are compared with autonomous systems generating electrical energy from renewable sources, alongside various types of refrigeration facility systems. Its objective is to assess the energy efficiency, financial feasibility, and environmental impact across four scenarios. Scenario 1 utilizes two R134a refrigeration units powered by the public grid. Scenario 2 employs a transcritical R744 (CO$_2$) system using grid electricity. Scenario 3 incorporates R744 and autonomous renewable energy. Scenario 4 employs R744 for refrigeration with seawater heat exchange and autonomous renewable energy sources. The findings favor Scenario 4, emitting 15,882 kg CO$_2$ eq with a 5-year return on investment. Autonomous electricity production in this scenario reduces emissions by 95%. Despite an initial cost of EUR 769,172.00, Scenario 3 demonstrates financial viability, contributing to energy sustainability. This autonomous production reduces emissions by 360,697 kg CO$_2$ compared to conventional systems, highlighting the positive impact of local renewable energy integration.

Keywords: CO$_2$; sustainable refrigeration; solar energy; wind energy; tidal energy

1. Introduction

The preservation of perishable foods, such as fish, plays a paramount role, requiring meticulous care from the moment of capture to the final consumption. Refrigeration facilities play a crucial role in this process and are known to consume a considerable amount of electrical energy, contributing significantly to the operational costs of companies [1]. The refrigeration sector stands out as one of the main energy consumers, representing 15 to 17% of the global electricity consumption. These high energy costs not only impact the profitability of operations but also increase the carbon footprint of organizations due to the greenhouse gas emissions associated with electricity production [2]. The integration of electricity production systems through renewable sources has become a viable possibility to reduce the carbon footprint and lower operational costs [3].

The integration between renewable energies and refrigeration systems is an area of research in constant evolution, marked by significant advances over the years. In the late 19th century, the first solar-powered refrigeration systems began to be developed, representing an initial milestone in this integration [4]. During the 20th century, as awareness of the importance of energy sustainability grew, pioneering studies exploring the use of wind and solar energy to power refrigeration systems emerged [5].

Advancements in technologies have demonstrated promising potential for integration with refrigeration systems. Hameed et al. [6] demonstrated the viability of solar refrigeration in Baghdad, emphasizing its effectiveness in reducing dependence on conventional

grids. Additionally, Yvon et al. [7] illustrate the positive integration of solar energy with vapor compression refrigeration systems. Roselli et al. [8] presented a study on a wind-driven heating, cooling, and electricity system for an office building in two Italian cities, emphasizing the effective integration of wind energy into heating and cooling systems, constituting a significant solution to achieve global environmental goals and guidelines. More recently, in recent years, there has been a significant expansion of research in this area. Studies have investigated the potential of other renewable energy sources, such as ocean energy, to power refrigeration systems, further expanding the options available for sustainable refrigeration in different industrial sectors [9].

This continuous evolution of the integration between renewable energies and refrigeration systems plays a crucial role in reducing energy consumption and promoting global energy sustainability. Cold storage facilities are known to play an essential role in food preservation. However, their high electricity consumption significantly impacts operational costs. The literature primarily emphasizes the positive aspects, neglecting evidence of comparisons between different types of refrigeration systems and the integration of various renewable energies. This study highlights, through comparison, the various advantages of integrating renewable energies with refrigeration systems.

The evolution of renewable energy technologies has brought the possibility of integrating sources such as wind, solar, and tidal energy into electricity generation, representing a crucial innovation to reduce operational costs and CO_2 emissions. In Tarrafal, Santiago, Cape Verde, the implementation of these sources aims to promote environmental sustainability and reduce expenses associated with refrigerated storage, leveraging favorable conditions of solar exposure, consistent winds, and strong tides.

2. Objective

The present study conducts a comparative analysis of four scenarios related to the installation of an integrated system in a cold storage facility located in Tarrafal, Santiago, Cape Verde. These scenarios encompass the sizing and selection of all mentioned systems. Technical, financial, and CO_2 emissions studies were conducted to evaluate the feasibility of integrating renewable energies to produce electricity aimed at operating the refrigeration systems. Solutions 3 and 4 represent the innovation of integrating renewable sources to meet the operational requirements of the proposed cold storage facility, offering benefits such as the reduction in CO_2 emissions and the promotion of local socioeconomic development. In summary, the article provides a comprehensive technical analysis, emphasizing the technical and financial viability of integrating renewable energy sources into electricity production for refrigeration systems.

3. Motivation

This work arises from the need to address the energy challenges faced by Cape Verde, a country that relies mainly on fossil fuels due to limited resources [10]. However, despite this dependence, Cape Verde exhibits considerable potential in renewable sources such as wind, solar, and ocean currents [11]. In this sense, this study aims to reinforce and promote, through comparisons between different systems, investment in electricity production systems based on renewable sources to power various industries, thereby reducing carbon footprint. Additionally, the work focuses on the locality of Tarrafal, on Santiago Island, known for its robust fishing industry, which faces challenges due to the lack of adequate infrastructure for the storage and preservation of products. In this context, the construction of cold storage facilities in Tarrafal is considered crucial, not only to address storage and preservation issues but also to boost local economic development through increased fish storage and processing capacity, waste reduction, job creation, and enhanced market competitiveness.

4. Materials and Methods

The search for clean and renewable energy sources has become a global priority due to concerns about climate change and the need to reduce CO_2 emissions. In this context, the use of wind, solar energy, and tidal energy has emerged as a viable and promising solution to meet the energy needs of various areas, including refrigeration.

The combination of wind and solar energy for food refrigeration offers a unique opportunity to promote sustainability in the food supply chain, especially in the city of Tarrafal, Santiago, Cape Verde. This leverages the excellent natural conditions of the region for generating energy from these renewable sources, reducing waste, and mitigating environmental impacts. An analysis of the climatic conditions in Tarrafal, Santiago was conducted, carried out through assessments of wind, solar, and tidal resources, considering variables such as topography and land availability. Based on these identified technical and climatic conditions, a comparative study was conducted among four proposed scenarios, varying the refrigeration systems and electricity production sources.

4.1. Conservation of Fish

The preservation of perishable food in the cold chain, from capture to consumption, highlights the importance of cold storage facilities [12]. These facilities aim to preserve food at controlled temperatures, preventing deterioration and contamination [13]. Cold storage facilities for fish, although crucial, are recognized as significant consumers of electrical energy, representing a substantial portion of operational costs. To mitigate these costs, imperative energy efficiency measures are necessary, including the use of more efficient equipment, adequate thermal insulation, and automation technologies for real-time monitoring and adjustment of conditions [14]. Additionally, it is crucial to implement energy management practices, involving measurement systems, setting consumption goals, and team training, as well as the use of renewable energy sources, to lower operational costs and carbon footprint. In this context, the present study highlights the importance of constant evolution in the search for more efficient systems in the preservation of products through comparisons between different proposed cold storage facilities.

4.2. Refrigeration System

The vapor compression refrigeration system is a well-established technology widely employed in heat transfer from a lower temperature source to a higher one based on the inverted Rankine cycle. This system comprises four main components: compressor, condenser, expansion device, and evaporator. The interconnection of these components enables the performance of fundamental thermodynamic processes: compression, condensation, expansion, and evaporation [15].

The vapor compression refrigeration cycle exhibits two distinct pressure levels: the condensation pressure (high pressure) and the evaporation pressure (low pressure). This pressure gradient allows for the phase change in the refrigerant, facilitating heat absorption or rejection. Consequently, the suction and liquid phases present different temperatures, hindering their energetic interaction in conventional installation methods [16].

In response to escalating environmental concerns and international commitments, carbon dioxide (CO_2) has emerged as a sustainable alternative in refrigeration, replacing traditional refrigerants like R134a in case studies [17]. Natural refrigerants such as CO_2 stand out as long-term options due to their non-flammability, non-toxicity, and suitability for vapor compression cycles. Additionally, their abundance in nature and neutrality concerning the greenhouse effect render them environmentally responsible choices. This technological advancement reflects a growing commitment to sustainable solutions in the refrigeration industry, aligning with global demands for more ecological practices [18].

The present comparative study exclusively focuses on refrigeration systems adopting the inverted Rankine cycle, varying between scenarios based on the type of refrigerant employed.

4.3. Wind Energy

Wind energy is a renewable energy source obtained from the force of the wind, widely recognized for its abundance, sustainability, and immediate availability. The most vigorous and persistent winds are found at altitudes exceeding one kilometer above the Earth's surface, rendering the installation of wind turbines in these layers unfeasible. Therefore, turbines are commonly positioned tens of meters above ground level [19]. However, the efficiency of these turbines is affected by factors such as terrain roughness, topography, and obstacles present in the installation area, making the identification and careful evaluation of suitable locations for their installation essential [20].

A typical wind energy production system comprises a wind turbine responsible for capturing the kinetic energy of the wind and converting it into electrical energy. The turbine's operation involves blades designed to capture wind energy, propelled by drag and lift forces. The movement of the blades is transmitted to a rotor, which rotates around a central axis. To increase the rotor's rotation speed, a gearbox is utilized, amplifying the speed, and transferring it to a generator. The generator then converts the mechanical energy into electrical energy through a power converter [21].

The electrical energy generated can be integrated directly into the public electricity distribution network through grid-tied systems or stored in batteries for autonomous use in isolated systems [22]. The power generated by a wind energy production system primarily depends on the wind speed and the turbine's operational capacity. Remarkably, refrigeration facilities for storage frequently adopt this type of system, where the produced energy is stored in batteries to ensure continuous supply during periods of low generation.

4.4. Photovoltaic Solar Energy

Photovoltaic solar energy is a technology that directly converts sunlight into electricity through solar panels, widely employed in residential and commercial systems [23]. These systems comprise essential components such as solar panels, inverters, and energy storage systems like solar batteries, enabling the storage of energy for future use and ensuring a continuous electricity supply, especially in off-grid systems [24]. The charge controller plays a crucial role in regulating the energy flow between the solar panels and the battery. Photovoltaic systems are categorized into grid-tied systems, off-grid systems, and hybrid systems, and it is essential to size them according to the energy needs of the installation [25]. The generated energy is initially converted into direct current (DC) by the photovoltaic modules, and a suitable inverter performs the conversion of this current into alternating current (AC) for use in residential and commercial applications.

4.5. Tidal Energy

Tidal energy, also known as marine current energy or oceanic energy, is a renewable form based on harnessing the kinetic energy of oceanic waters, influencing ecosystems, nutrients, and climatic patterns, [26]. Originating from surface and deep currents, this energy stands out for its renewability, predictability, and low carbon emissions, minimizing impacts in urban areas [27]. Turbines convert kinetic energy into electricity, comparable to the principle of wind energy, but with water density approximately 800 times higher, providing greater generation capacity per unit area compared to wind energy [28]. The oceanic location of these currents minimizes visual and sound impacts on coastal communities.

5. Fish Refrigerated Warehouse

5.1. The Cold Store Facility

The proposed cold storage facility will be situated in the bay of the city of Tarrafal, in Santiago, Cape Verde (Figure 1a). The proposed cold storage facility (Figure 1b) will comprise a chamber for frozen product storage, a chamber for refrigerated products, and a buffer area for the reception and dispatch of products.

(**a**)   (**b**)
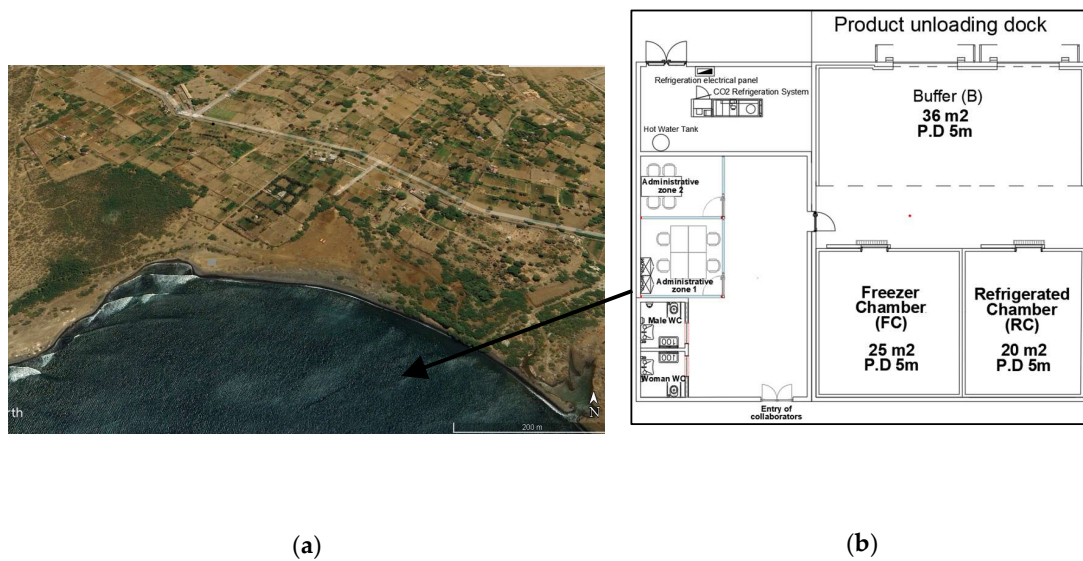
Figure 1. Localization (**a**) and layout (**b**) for the facility.

5.2. Thermal Loads

A thermal load for the sizing of the current fish refrigerated warehouse project was developed and is essential to consider a variety of factors that will influence the performance and efficiency of the refrigeration system. Table 1 presents these factors.

Table 1. Considered parameters for thermal loads.

Parameter	B	RC	FC
Thermal insulation thickness (mm)	100	100	100
Ambient temperature on internal corridor (°C)	15	15	15
Number of people	3	2	2
Lighting lamps (kW)	0.256	0.128	0.128
Transport and logistics equipment (kW)	1.450	1.450	1.450
Product density (kg/m^3)	400	350	600
Product inlet temperature (°C)	8	5	−5
Evaporator operating time	16	16	16
External ambient temperature (°C)	35	35	35
Heat flux (W/m^2)	8	8	8
Product storage temperature (°C)	2	0	−25
Thermal conductivity of the insulation (W/(mK))	0.0207	0.0207	0.0207

Determining the thermal loads of each refrigerated space is crucial for the proper sizing of refrigeration systems. This process ensures the maintenance of suitable conditions for product storage. Equations (1)–(4) represent the partial thermal loads considered in the sizing process of refrigerated spaces. Equation (1) describes the calculation of thermal load due to conduction through walls, influenced by various factors such as the thermal conductivity of the wall material, its thickness, and the temperature difference between both sides of the wall [29].

$$\dot{Q}_p[kW] = \frac{(T_{int} - T_{ext})}{R_{project}}$$

(1)

where

T_{int}—Internal temperature (°C)

T_{ext}—External temperature$(°C)$
$R_{project}$—Thermal resistance of the wall $(°C/kW)$

Equation (2) calculates the thermal load resulting from the introduction of the product under different thermodynamic conditions compared to the internal air of the refrigeration chamber [30]. This thermal load pertains to the amount of heat introduced by the stored product into the refrigerated space.

$$\dot{Q}_{prod}\ [kW] = \dot{m}_{rot.}C_P\left(T_{in,prod} - T_{int}\right) \tag{2}$$

where

$T_{in,prod}$—Product inlet temperature$(°C)$
$\dot{m}_{rot.}$—Product flow into the coldchamber $\left(\frac{kg}{s}\right)$
C_P—Specific heat of the product before freezing $\left(\frac{kJ}{kg \cdot K}\right)$

Equation (3) calculates the internal thermal loads, which refer to the heat generated within a space by sources such as occupants, lighting, and equipment [31]. These loads have a direct impact on the ambient temperature and the performance of refrigeration systems. The thermal load due to occupants is determined by the heat from human metabolism, varying according to the number of people present. The thermal load from lighting is the heat emitted by light sources, while the thermal load from equipment is the heat generated by devices in operation.

$$\dot{Q}_{int}[kW] = \dot{Q}_{occupants} + \dot{Q}_{lighting} + \dot{Q}_{equipment} \tag{3}$$

where

$\dot{Q}_{occupants}$—Thermal loads from occupants (kW)
$\dot{Q}_{lighting}$—Thermal loads from lighting (kW)
$\dot{Q}_{equipment}$—Thermal loads from equipment (kW)

Equation (4) calculates the thermal load due to air infiltrations into the refrigerated space within the chamber [32]. This parameter is essential in determining the total heat entering the refrigerated environment through undesired air infiltrations.

$$\dot{Q}_{inf}[kW] = \dot{m}_{renov}E_{ar} \tag{4}$$

where

$\dot{m}_{renov}$—Infiltration air flow$\left(\frac{kg}{s}\right)$
E_{ar}—Specific energy of air $\left(\frac{kJ}{kg}\right)$

In Table 2, the Cooling Power of the refrigerated warehouse is presented.

Table 2. Thermal loads and refrigeration capacity of refrigerated spaces.

Thermal Load	FC	RC	B
Conduction (kW)	1.23	0.47	2.08
Product (kW)	4.02	0.77	4.13
Internal (kW)	0.47	0.44	0.82
Infiltration (kW)	1.61	0.19	1.03
Cooling Power (kW)	12.1	3.1	13.3

It is observed that the values obtained for each type of load fall within a range considered normal for the typical dimension of the chamber. This suggests that the thermal loads are in line with expectations for the proper sizing of the refrigeration system for each specific space.

6. Innovation Solutions

The highlighted scenarios in this study, referred to as Scenario 3 and Scenario 4, stand out for the adoption of a transcritical booster refrigeration system utilizing the refrigerant R744. The electrical energy required to facilitate the operations of the refrigeration warehouse is provided by an autonomous renewable energy generation system, sourced from renewable energy such as wind power, photovoltaic solar energy, and marine currents.

6.1. R744 (CO2) Booster Refrigeration Systems

A conventional CO_2 booster refrigeration system, commonly found in supermarkets, is depicted in Figure 2, and comprises four pressure sections: high, intermediate, medium, and low [33]. Low-pressure compressors are responsible for extracting superheated vapor from low-temperature evaporators. Subsequently, this vapor is compressed by medium-temperature compressors until it reaches the discharge pressure of the gas cooler, where heat is dissipated to the external environment [34]. To control the pressure of the transcritical refrigerant fluid after the gas cooler, a transcritical high-pressure valve is employed. Before entering the liquid receiver, R744 is throttled into a liquid–gas mixture and separated into gas and liquid phases. The saturated liquid refrigerant is then distributed to the medium and low-temperature evaporators, where it is expanded through different valves to reach the corresponding pressure [35]. To enhance energy efficiency, heat recovery from the compressor discharge gas has been implemented, allowing the recovery of sanitary hot water through a plate heat exchanger unit located between the outlet of the high-pressure compressor and the gas cooler pressure.
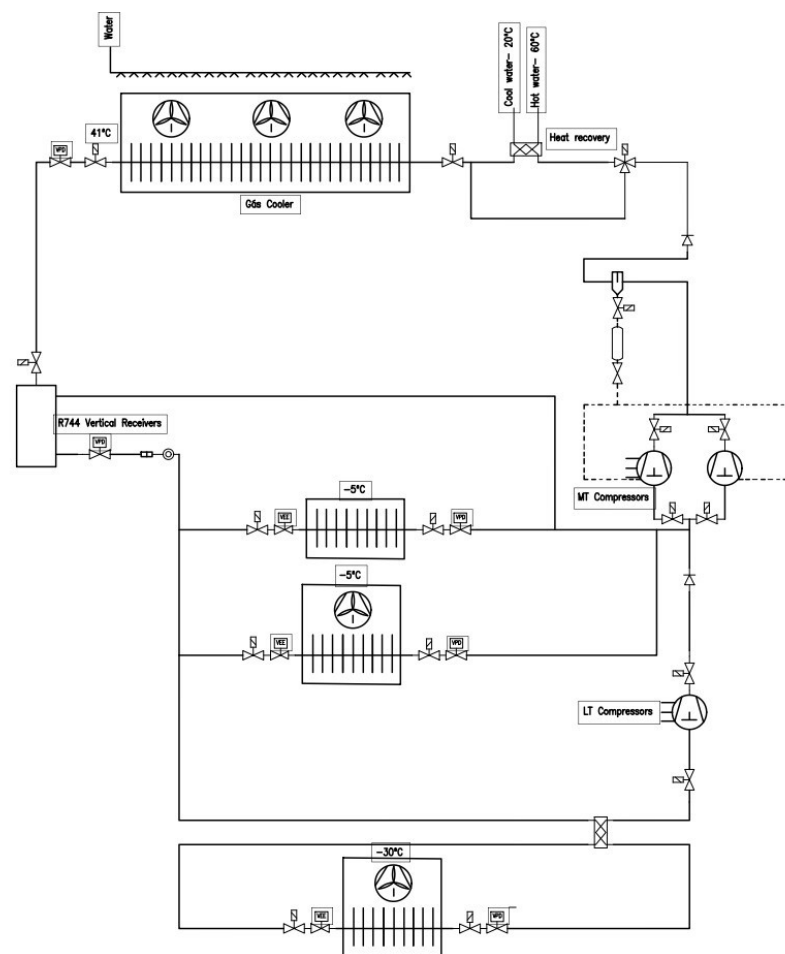

Figure 2. Principle diagram for the refrigeration system.

Figure 3 illustrates the Mollier diagram corresponding to the principle diagram of the refrigeration system presented. The blue coloration is associated with the low side refrigeration cycle, known as the subcritical cycle, while the red color represents the medium-pressure refrigeration cycle, referred to as the transcritical cycle. In the low temperature (LT) stage, the steps occur as follows: Compression (1–2): the refrigerant vapor is compressed, resulting in an increase in its pressure and temperature. Evaporation (11–12): the refrigerant absorbs heat from the surroundings, changing its state to vapor.
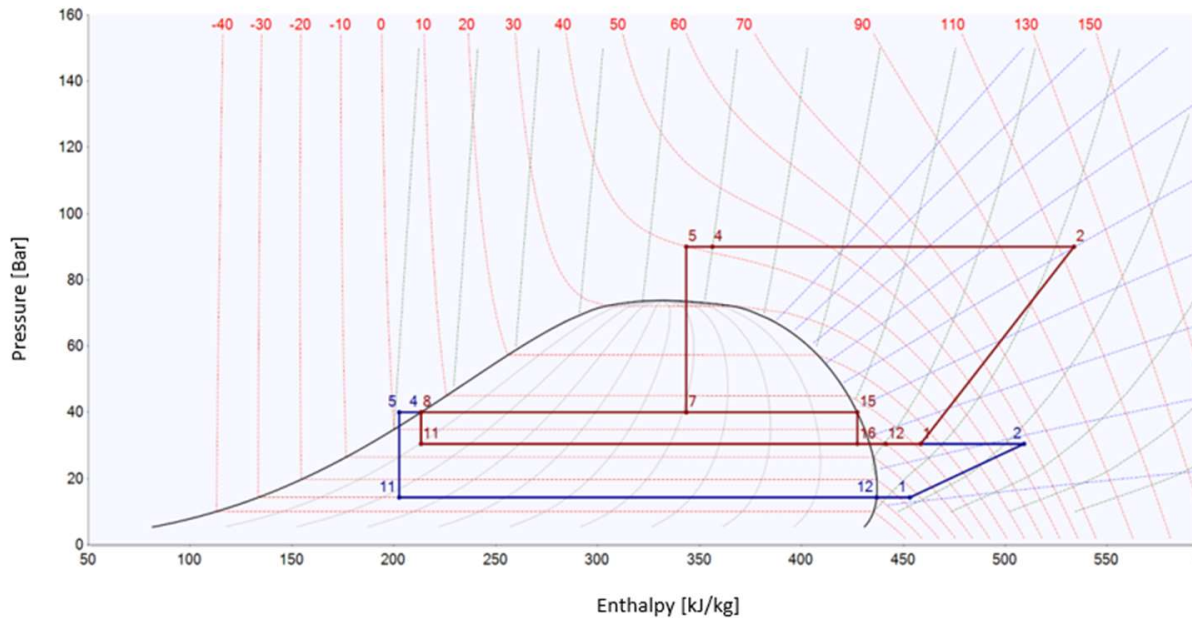
Figure 3. Mollier diagram of the refrigeration installation.

Superheating (12–1): the vapor is further heated. Expansion (4–11): the refrigerant expands, reducing both its pressure and temperature. Meanwhile, in the medium-temperature (MT) stage, the steps follow this pattern: Compression (12–2): the refrigerant vapor from the low-temperature stage is compressed once again. Gas cooling (2–4): the compressed vapor loses heat, transforming into a liquid. Expansion to Intermediate Pressure (4–7): the refrigerant liquid expands to an intermediate pressure. Outlet of liquid from the intermediate tank (7–8): the refrigerant liquid is directed out of the tank. Expansion to evaporation pressure (15–16): again, the liquid expands, this time to reach the necessary pressure for evaporation. Evaporation (11–16): the liquid absorbs heat and transforms into vapor. Outlet of gas from the intermediate tank (7–15): the refrigerant vapor is directed out of the tank. Superheating (16–12): the vapor, already completely transformed, is further heated before starting a new compression cycle. These steps outline the cycle through which the refrigerant passes to absorb and dissipate heat, enabling the operation of the refrigeration system.

6.2. Electrical Characteristics for the System

Table 3 presents, as an example, the calculated values of the main electrical parameters of the proposed warehouse for Scenario 3. The electrical characteristics of the system were determined by considering factors such as the total electrical load, the type of electrical equipment, the voltage of the electrical grid, and the distance between the points of consumption and the power source. Active power, reactive power, and apparent power were analyzed.

Table 3. Electric cold panel parameters of Scenario 3.

Parameters	Electric Cold Panel
Service Current (A)	171.07
Phase current R (A)	116.67
Phase current S (A)	119.47
Phase current T (A)	116.67
Active Power (kW)	69.95
Apparent Power (kVA)	81.44
Reactive Power (kVar)	41.39
Amplification Coefficient	1.20
Simultaneity Coefficient	1
Utilization Current (A)	169.76
Power Factor (cos φ)	0.86

6.3. Photovoltaic Solar System

6.3.1. PV Calculations

A grid-tied photovoltaic system was considered to optimize the utilization of available solar energy, seamlessly integrating it into the electricity supply for refrigeration facilities. Solar panels convert solar energy into electricity, which is directly utilized by the electrical installation of refrigeration units. The choice of this system was motivated by the need for continuous electrical supply and the distance to the power source. The system's efficiency depends on the effectiveness of its individual components, determined by a detailed technical analysis that considered both the overall efficiency and the effectiveness of the primary energy conversion devices.

The system sizing considered not only its overall efficiency but also the effectiveness of the primary energy conversion devices. In this context, Equation (5) was employed to present the considered effectiveness of these devices, specifically the performance of the cable (0.98), the solar charge controller (0.97), the battery performance (0.9), and the inverter performance (0.98) [36,37].

$$\eta_{ss}[\%] = \eta_c \cdot \eta_r \cdot \eta_b \cdot \eta_i \tag{5}$$

where

η_C—Cable performance
η_r—Solar charge controller performance
η_b—Battery performance
η_i—Inverter Performance

The photovoltaic panel has a power capacity capable of ensuring the satisfaction of half of the daily energy consumption of the refrigeration facility. Furthermore, the sizing was carried out for the month of December, which represents the most unfavorable period in terms of solar availability in the city of Tarrafal in Santiago, Cape Verde. This month is characterized by a reduced number of hours of sunlight equivalent to the standard radiation of 1000 W/m^2. Equation (6) defines the maximum power that the photovoltaic panel array should have [38].

$$P_{PV}[kWh] = \frac{Load}{\eta_{ss} \cdot PHS} \tag{6}$$

PHS—Peak Solar Hours (hours/day)

The determination of the number of modules per series (Np) and the number of series (NS) is of paramount importance in determining the quantity of photovoltaic panels required. Typically, it is recommended that the operating voltage increases according to the

daily load consumption. For daily loads exceeding 4 kWh, the choice of 48 V is advisable, resulting in reduced losses in the system [39].

$$N_S = \frac{V_{CC}}{V_{mpp}}$$ (7)

V_{mpp}—Peak Power Voltage (V)

$$N_p = \frac{P_{PV}}{N_S \cdot P_m}$$ (8)

P_m—Nominal power of the selected panel.

The data regarding the electrical capacity generated by the panels and the efficiency of the energy conversion system are recorded in Table 4. This table not only provides the calculated values of a load of 42 kW and a system efficiency of 0.84 but also presents the levels of monthly and daily irradiation, along with the daily hours of solar exposure. This information was obtained from the European Commission [40] and is crucial for understanding and analyzing the feasibility of the energy system under consideration.

Table 4. Photovoltaic system specifications.

Parameters	Value
Load (kW)	42
System Efficiency	0.84
Monthly Irradiance (kWh/m^2)	159.73
Daily Irradiance (kWh/m^2)	5.15
Hours of Sunlight per Day	5.15

6.3.2. PV Panel Selected Model

The sizing of the photovoltaic panels assumed of the available area on the roof of the cold storage facility designated for installation (180 m^2). Considering the physical dimensions of the selected panel, model RT8I-M560—Restarsolar (2.272 m × 1.134 m), and considering the spacing between panels (60 mm) to account for shading, this resulted in a total of 51 panels. To calculate the total power generated by the panels, the solar irradiance at the optimal angle of 12° during the month of December in the city of Tarrafal de Santiago was estimated based on data provided by the European Commission, yielding the total power produced by the photovoltaic panels. Table 5 presents the values of the main parameters of the photovoltaic solar installation.

Table 5. Parameters of the photovoltaic solar installation.

Parameters	Value
Individual Panel Power (kW)	0.56
Number of Panels	51
Hours of Sunlight per Day (PHS) (h/day)	5.2
System Efficiency (%)	84
Total Daily Peak Power (kWh)	123.5
Instantaneous Peak Power (kW)	5.14

6.4. Wind Turbine

6.4.1. Wind Turbine Calculations

A wind-based electricity generator will convert wind energy to electricity energy; it follows the energy reservation principle. Wind turbines partly convert wind energy into electricity energy. The theoretical power available in a wind stream is given by Equation (9) [41].

$$P = \frac{1}{2}\rho\, AV^3$$ (9)

where

A—Cross-sectional area of rotor (m^2);
ρ—Density of air stream (kg/m^3);
V—Velocity of wind stream (m/s);
P—Generated energy per unit time (W).

Actual power produced by a rotor would be decided by the efficiency with which this energy transfer from the wind to the rotor takes place. The efficiency is usually termed as the power coefficient Cp, as in Equation (10) [42].

$$Cp = \frac{2\,P_T}{\rho\,AV^3} \tag{10}$$

where

P_T—Power developed by the turbine (W);
C_p—Coefficient that depends on many factors such as the profile of the rotor blades, blade arrangement and setting, etc. (dimensionless).

Wind resource analysis focuses on the wind's energy content, determined by air density and velocity, variables influenced by atmospheric pressure and temperature, which are altitude-dependent [43]. The theory of the ideal actuator disk, based on assumptions like homogeneous, incompressible, and steady-state fluid flow, is applicable to various types of wind turbines [44]. The maximum achievable efficiency is 59% due to the requirement of continuous airflow, capturing 100% of the energy would halt wind movement, rendering energy extraction impossible [45]. Optimal balance is achieved by slowing the wind sufficiently to maintain a steady flow through the turbine.

6.4.2. Wind System Selection

The selection of the wind turbine was based on the analysis of wind conditions at the project site, using climatic data provided by Meteoblue for the city of Tarrafal, covering the last 30 years. Wind speed and direction were assessed at a height of 64 m above the ground. A design speed of 26 km/h (in Figure 4) was taken into consideration, indicating significantly high values, and suggesting highly favorable conditions for the utilization of wind energy.
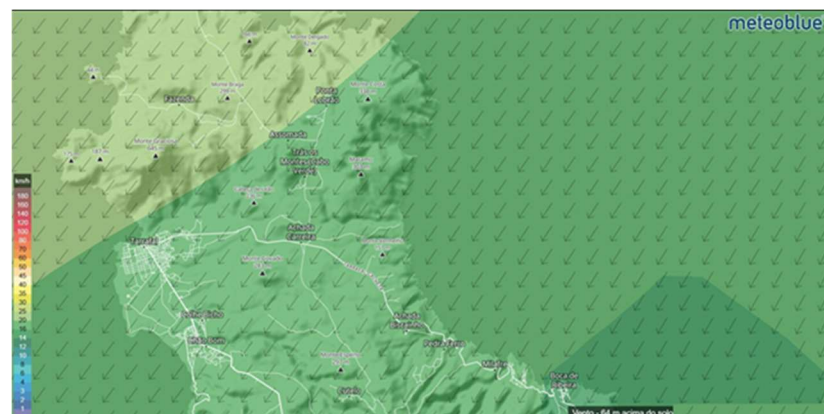

Figure 4. Observed Wind Speed and Direction [46].

Two E-3120 wind turbines with a 50 kW capacity manufactured by Endurance Power were selected. Despite the nominal power of 50 kW, the appropriate power for the specific project conditions will be 27.5 kW.

6.5. Tidal Energy

An analysis of marine current velocities near the Tarrafal Bay in Santiago was conducted at the installation site using data provided by Meteoblue (see Figure 5). An estimated average marine current velocity of 6 km/h was considered, signifying a favorable speed for harnessing energy from marine currents. The turbine would be positioned at a depth of 30 m below the sea surface. Based on this, the estimated average velocity at this depth was determined, resulting in a value of 2.34 m/s. An integrated system was selected, featuring the axial turbine POSEIDE 154 from Guinnard Energie, renowned for its nominal power of 10 kW.
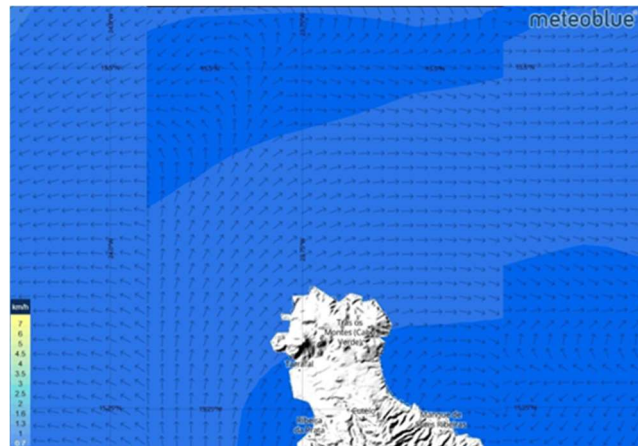
Figure 5. Marine current velocities in Tarrafal Bay, Santiago [47].

6.6. Schematic Diagram

Figure 6, depicting the Scenario 3 diagram, provides a comprehensive view of the system structure, highlighting the integration of renewable energy sources. This diagram showcases the seamless integration of wind energy (on the right), photovoltaic solar energy, and tidal energy (on the left), offering a detailed visual representation of these energy solutions. This schematic representation simplifies the visual understanding of the interconnection among various energy sources, demonstrating their synergy and complementarity within the global energy system context.
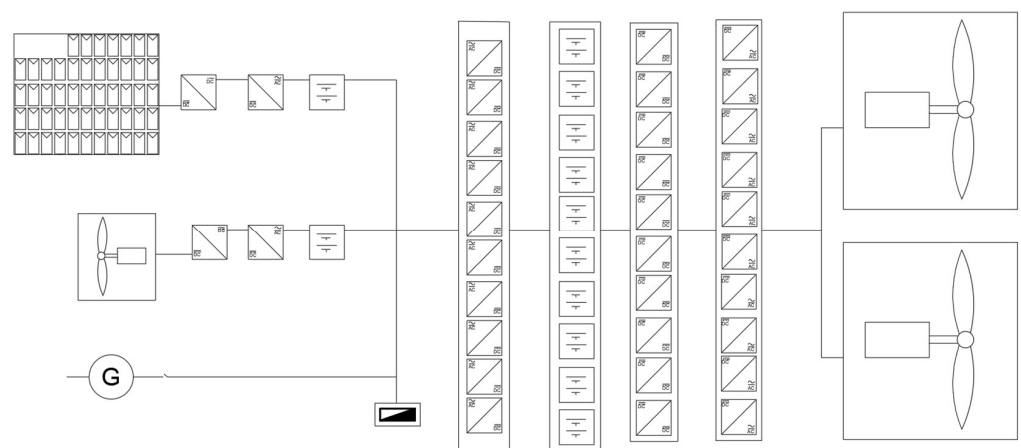

Figure 6. Integrated energy system schematic diagram.
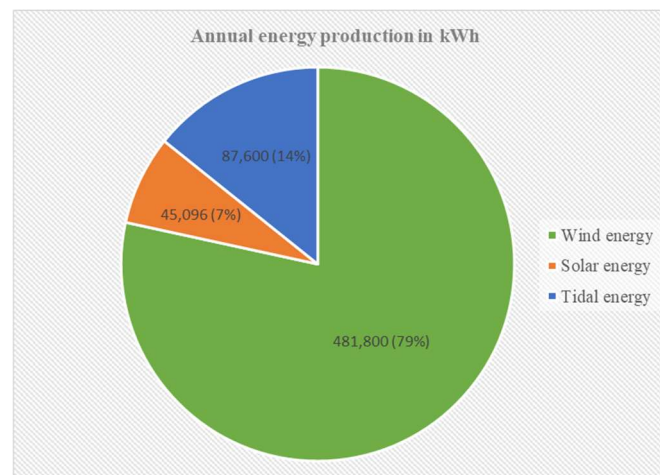
7. Results

7.1. Distribution Energy Production of Innovation Solutions

Figure 7 presents the daily and annual contribution analysis for Scenario 3, spanning a specific day in December and the entire year. It is observed that most of the contribution comes from wind energy (79%), followed by tidal energy (14%), and solar energy (7%).
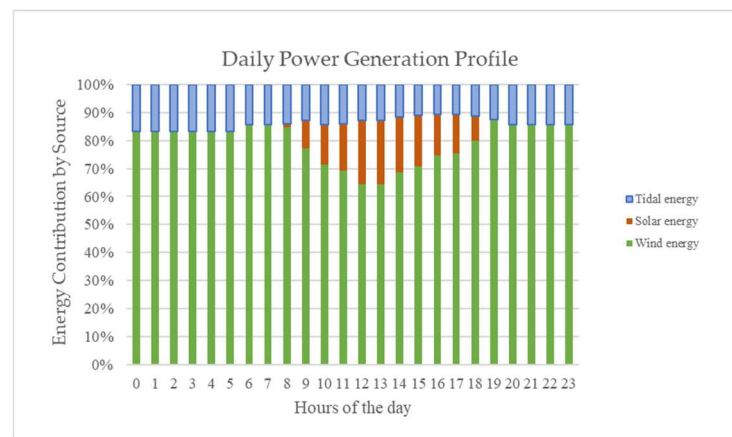
Figure 7. Energy contribution.

The analysis of the annual contributions from solar, wind, and tidal energy sources reveals that the predominant contribution is from wind energy (481,800 kWh—79%), followed by tidal energy (87,600 kWh—14%), and solar energy (45,097 kWh—7%), (See Figure 8).

Figure 8. Energy sources.

The results highlight the predominance of wind energy as the primary renewable energy source in this context, surpassing expectations. With a significantly higher contribution of 79%, compared to other sources such as solar energy (7%) and tidal energy (14%), there is considerable potential for wind energy generation in the region and in the analyzed system. Although tidal and solar energy also play important roles, their contributions are considerably smaller compared to wind energy. Solar energy production is limited to a restricted daily period of approximately 9 h due to the lack of sunlight during the rest of the day. Meanwhile, tidal energy remains constant, with low fluctuations in its production over time. This distribution of contributions underscores the need for continuous investments in wind energy technologies and infrastructure, maximizing its potential and promoting the transition to more sustainable and environmentally friendly energy sources.

7.2. Considered Scenarios

The aim of this comparative study is to assess and compare refrigeration systems, along with their associated electrical power supply systems, with the purpose of identifying the most viable solution from both environmental and financial perspectives. The primary objective of this study is to promote compliance with the goals set forth in relevant international agreements, including the Kyoto Protocol (1997), the Montreal Protocol (1987), and

the Paris Agreement (2015). To achieve this, four distinct scenarios will be examined, delineated to highlight relevant specifics, and enable comparison among different approaches. Through this comprehensive analysis, the aim is to contribute to the adoption of more sustainable and efficient practices, aligned with the objectives of emission reduction and climate change mitigation established in the international agreements and protocols.

Scenario 1

In the scope of the first analyzed scenario, a refrigeration system comprising two distinct refrigeration plants, both operating with the refrigerant R134a, was studied. One of these plants was specifically designed for storing frozen products, while the other was intended for refrigerated products. Each of these plants was meticulously engineered to meet the specific requirements of freezing and cooling, respectively. In this case (Figure 9), the electrical energy required for the operation of the refrigeration warehouse is sourced from the public electrical grid. There is no form of autonomous electrical energy production from renewable sources associated with this scenario.
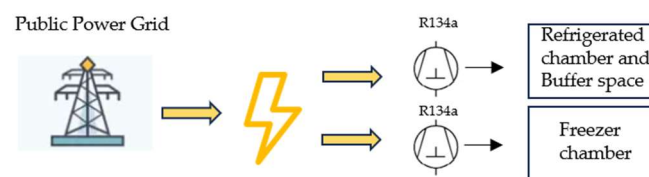
Figure 9. Schematic representation of Scenario 1.

Scenario 2

In Scenario 2, a transcritical booster refrigeration system using refrigerant R744 (CO_2) was considered. In this specific case (Figure 10), the electrical energy required for the operation of the refrigeration warehouse is sourced from the public electrical grid. There is no form of autonomous electrical energy production from renewable sources associated with this scenario.
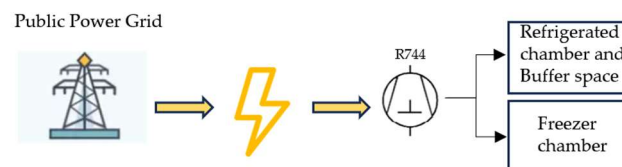
Figure 10. Schematic representation of Scenario 2.

Scenario 3

In Scenario 3, a transcritical booster refrigeration system utilizing refrigerant R744 was considered. The electrical energy required for the operation of the refrigeration warehouse is supplied by an autonomous renewable energy production system, sourced from renewable energy such as wind power, photovoltaic solar energy, and marine currents (Figure 11).
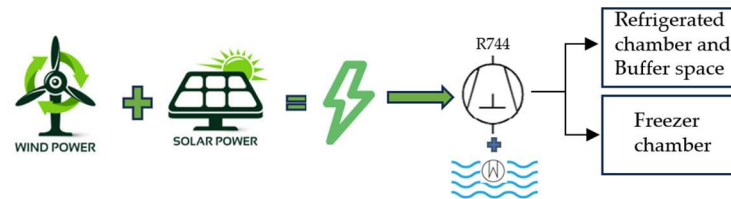
Figure 11. Schematic representation of Scenario 3.

Scenario 4

In Scenario 4, a subcritical booster refrigeration system using refrigerant R744 was considered. Due to the climatic conditions in Tarrafal, Cape Verde, where external temperatures can reach up to 35 °C, operating a subcritical system under these circumstances is

not feasible. Therefore, it was determined that the refrigerant cooling is achieved through heat exchange with seawater near the refrigeration warehouse. In this specific context (Figure 12), the electrical energy required to operate the refrigeration warehouse is obtained through an autonomous renewable energy production system, utilizing wind and photovoltaic solar energy sources.

Figure 12. Schematic representation of Scenario 4.

7.3. Coefficient of Performance

Table 6 presents a synthesis of essential information regarding the cooling capacity, hot water recovery, electrical power of the refrigeration unit, Coefficient of Performance (COP), total electrical power of the installation, and annual energy consumption for each analyzed case. These data played a crucial role in comparing the studied scenarios, allowing for a deeper understanding of the performance and energy efficiency of each configuration. The analysis of these values is pivotal in identifying the most effective and sustainable solution concerning energy consumption and cooling capacity. The COP was calculated based on the electrical power of the refrigeration unit (kWe), cooling capacity (kW), and hot water recovery (kW). The cooling capacity (kW) remains constant across all considered scenarios, while the hot water recovery (kW) varies depending on the scenario under study. As for the values of the electrical power of the refrigeration unit (kWe), these correspond to the power of the selected equipment.

Table 6. Comparative analysis of refrigeration systems.

Case Study	Cooling Capacity (kW)	Hot Water Recover (kW)	Electrical Power of Refrigeration Unit (kWe)	COP	Total Electrical Power of the Installation (kWe)	Total Annual Energy Consumption (kWh)
Scenario 1	28.48	0	14.33	1.99	54.264	475,352
Scenario 2	28.80	10.32	29.87	1.30	69.952	613,200
Scenario 3	28.80	10.32	29.87	1.30	69.952	613,200
Scenario 4	28.80	10.32	12.86	3.02	50.801	445,016

Upon analyzing Table 6, it is noteworthy that Scenario 4 exhibits the highest Coefficient of Performance (COP), reaching a value of 3.02. This data suggests a remarkably superior efficiency in utilizing electrical energy for refrigeration production. Furthermore, it is pertinent to emphasize that Scenario 4 features the lowest electrical power, totaling 50.801 kWe, making it the lower value among the analyzed scenarios. Conversely, Scenario 1 demonstrates a substantially lower COP than Scenario 4. This decrease in efficiency is attributed to the absence of a heat recovery system for hot water, resulting in a reduction in COP compared to the other scenarios. In contrast, Scenarios 2 and 3 present a COP of 1.30, indicating an efficiency of less than half when compared to Scenario 4. These results are in line with values obtained in other studies, such as those conducted by Sengupta et al. [48]. Consequently, based on the presented data, it is concluded that Scenario 4 emerges as the most efficient system. This scenario not only presents the highest COP but also boasts the lowest total installed electrical power. This translates to significant energy efficiency and lower electricity consumption to provide the same thermal capacity compared to the other scenarios.

7.4. Costs and Payback

The economic performance of the study was evaluated over a 10-year period through a financial analysis. This assessment considered crucial parameters such as the initial investment, annual energy costs, generated savings, and the impact of inflation. Regarding the initial investment, the total cost of the refrigeration facility was considered, encompassing the cost of the autonomous electricity production system and the refrigeration installation. Annual energy costs included the yearly expenses on electrical energy, adjusted according to the electrical power required for each study scenario. The annual savings generated relate to the reduction in electrical energy expenses resulting from the use of autonomous energy production systems, eliminating the need to acquire electricity from the public grid in this scenario.

Analyzing Table 7, it is evident that scenarios with higher initial investments (Scenarios 3 and 4) demonstrate better financial viability due to the utilization of autonomous systems to produce electrical energy from renewable sources. Despite the initial investments of EUR −769,172.00 in Scenario 3 and EUR −713,524.00 in Scenario 4, these scenarios show considerably robust accumulated balances after 10 years, EUR 1,498,380.53 in Scenario 3 and EUR 932,100.85 in Scenario 4. Scenario 3 stands out with the best payback period, achieving 4 years due to high annual energy savings. Although Scenario 4 has a longer payback period (5 years) compared to Scenario 3, it represents a more secure initial investment. The accumulated balances in Scenarios 1 and 2 are negative as these systems utilize electricity from the public grid, resulting in a negative cash flow over the years, with accumulated balances of EUR −1,757,806.72 and EUR −2,331,126.53 for Scenario 1 and 2, respectively. Scenarios 1 and 2 have an infinite payback period due to the absence of energy savings over the years.

Table 7. Financial study for different scenarios.

Case Study	Initial Investment (EUR)	Energy Savings (EUR) after 10 Years	Accumulated Balance (EUR) after 10 Years	Payback Period
Scenario 1	−41,000.00	−1,757,806.72	−1,620,643.21	∞
Scenario 2	−63,574.00	−2,267,552.52	−2,331,126.53	∞
Scenario 3	−769,172.00	2,267,552.52	1,498,380.53	4
Scenario 4	−713,524.00	1,645,624.84	932,100.85	5

7.5. CO_2 Emissions

Table 8 illustrates a comparative study of carbon dioxide (CO_2) emissions associated with various electricity production systems in the four scenarios examined. The CO_2 emissions were determined considering the annual amount of electricity produced by autonomous renewable energy generation systems and electricity purchased from the public grid. This calculation is based on the CO_2 equivalent emissions associated with each autonomous electricity production system, as well as the CO_2 equivalent emissions from Cape Verde public grid, expressed in kilograms of CO_2 equivalent (kg CO_2 eq.). Values for electricity from Cape Verde's public grid (0.623 kg CO_2 eq./kWh), wind systems (0.034 kg CO_2 eq./kWh), solar photovoltaic systems (0.05 kg CO_2 eq./kWh), and tidal turbines (0.034 kg CO_2 eq./kWh) were considered [49–51]. The total value of CO_2 emissions associated with each scenario is determined by summing the CO_2 equivalent emissions from each autonomous electricity production system, combined with the CO_2 equivalent emissions from electricity purchased from Cape Verde's public grid. Each scenario was assessed regarding its contribution to the total CO_2 emissions, allowing for a comparative analysis of environmental impacts related to different electricity sources.

Table 8. CO_2 emissions in different scenarios studied.

Scenario Study	Annual Energy (kWh)	CO_2 Emission Grid Electricity (kgCO$_2$ eq./kWh)	CO_2 Emission Wind System (kgCO$_2$ eq./kWh)	CO_2 Emission Solar Photovoltaic System (kgCO$_2$ eq./kWh)	CO_2 Emission Tidal Turbines (kgCO$_2$ eq./kWh)	Total Emission (kgCO$_2$ eq.)
Scenario 1	475,352	0.623				296,316.94
Scenario 2	613,200	0.623	-	-	-	382,246.31
Scenario 3	613,200	-	0.034	0.050	0.034	21,549.32
Scenario 4	445,016	-	0.034	0.050		15,882.44

Scenario 1 adopts electricity from the public grid to supply power to the refrigerated warehouse, resulting in CO_2 emissions of 296,316.94 kgCO$_2$ eq. It is noteworthy that, besides being a system with high CO_2 emissions, the refrigerant (R134a) used in the refrigeration system is prohibited in various countries, including Cape Verde, due to its high global warming potential, rendering its widespread use unfeasible [52].

In Scenario 2, exclusive reliance on electricity from the public grid in Cape Verde results in substantial CO_2 emissions totaling 382,246.31 kgCO$_2$ eq, attributed to the high CO_2 intensity associated with the country's public grid. Scenario 3 incorporates an autonomous electricity production system through wind, solar, and tidal energy, resulting in considerably lower emissions totaling 21,549.32 kgCO$_2$ eq. Scenario 4 exhibits the lowest emissions among the scenarios, almost identical to Scenario 3, totaling 15,882.44 kgCO$_2$ eq.

Comparing the total CO_2 emissions in each scenario, it becomes evident that autonomous electricity production systems (Scenarios 3 and 4) are the most environmentally sustainable in terms of CO_2 emissions, providing a significant reduction compared to reliance on the public grid (Scenarios 1 and 2). The implementation of an autonomous electric power generation system resulted in a 95% reduction in CO_2 emissions when compared to the electricity consumed from the public grid. This analysis underscores the critical importance of investing in renewable energy sources, such as wind and solar power, to mitigate CO_2 emissions and contribute to more ambitious environmental goals, at the expense of reliance on fossil fuels.

8. Discussion

Analyzing the comparative scenarios, the conclusion is that Scenario 4 emerges as the most advantageous hypothesis. This assessment is based on various criteria, namely, its lower initial investment compared to Scenario 3, a short payback period, a higher Coefficient of Performance (COP) compared to other scenarios, and a significant reduction in CO_2 emissions (95%) compared to Scenario 2. This performance is attributed to the implementation of an autonomous electricity production system powered by renewable sources.

Scenario 1 is the least favorable, discouraged due to the use of R134a with a high global warming potential (GWP = 1430), rendering it obsolete. Additionally, it has an infinite payback period and high CO_2 emissions. Scenario 4 stands out as the most favorable, integrating both environmental and financial features, as stated before. Scenarios 2 and 3 benefit from the adoption of a widely used refrigeration system, with heat recovery for hot water. Financially, Scenario 3 represents the highest initial investment among all studied Scenarios, while Scenario 2 presents the lowest initial investment. However, Scenario 3 provides a superior financial return for the same study period due to higher energy savings. Regarding CO_2 emissions, Scenarios 1 and 2 proved unfeasible, while Scenarios 3 and 4 are favorable. Considering all the advantages presented, it becomes evident that Scenarios 3 and 4 are the most viable choices from both financial and environmental perspectives.

9. Conclusions

The financial analysis confirms the viability of Scenario 3, despite the higher initial investment of EUR −769,172.00. Positive returns are achieved rapidly, with the expectation of recovering the investment from the 4th year onwards for the cold storage facility instal-

lation. Over a decade, the accumulated balance of EUR 1,498,380.53 substantially surpasses other scenarios studied, demonstrating the efficiency.

The study of CO_2 emissions highlights the significance of adopting an autonomous system for electricity production from renewable sources, as opposed to electricity sourced from the public grid, which is heavily reliant on fossil fuels. The equivalent CO_2 emission value for Scenario 3 is 21,549.32 kgCO_2 eq., compared to Scenario 2 (public grid electricity), which totals 382,246.31 kgCO_2 eq. This represents a 95% reduction for the same refrigeration system used. Diversifying these sources and maintaining a balanced energy production strategy mitigate the risks associated with adverse weather conditions, ensuring a continuous and reliable energy supply.

The results from Scenarios 3 and 4 serve as clear indicators of the financial viability of these studies, contrasting positively with Scenarios 1 and 2. This finding strongly encourages the integration of refrigeration systems with electricity production systems from renewable sources. Such integration not only promotes the adoption of sustainable practices but also plays a significant role in achieving the goals established by the Kyoto, Montreal, and Paris Protocols.

The analysis of the results underscores the crucial importance of implementing autonomous renewable energy systems as integral parts of strategies aimed at promoting sustainability. By diversifying energy sources, not only are the risks associated with fossil fuel dependency mitigated but also a more stable and reliable energy supply is ensured. Additionally, this approach reinforces the global imperative of sustainable practices, which play a fundamental role in reducing greenhouse gas emissions and mitigating climate change. In summary, the implementation of autonomous renewable energy systems represents a substantial step towards achieving a more sustainable energy matrix and socio-economic development in Tarrafal and beyond. This study highlights the importance of adopting innovative and sustainable approaches in the energy sector, not only to meet present demands but also to ensure a more prosperous and equitable future for future generations.

References

1. Arteconi, A.; Polonra, F. Demand side management in refrigeration applications. *Int. J. Heat Technol.* **2017**, *35*, S58–S63. [CrossRef]
2. Tassou, S.A.; Ge, Y.; Hadawey, A.; Marriott, D. Energy consumption and conservation in food retailing. *Appl. Therm. Eng.* **2011**, *31*, 147–156. [CrossRef]
3. Lu, Y.; Huo, E. Viewpoints on the Refrigeration by Renewable Energy. *Front. Energy Res.* **2022**, *10*, 928187. [CrossRef]
4. Al-Yasiri, Q.; Szabó, M.; Arıcı, M. A review on solar-powered cooling and air-conditioning systems for building applications. *Energy Rep.* **2022**, *8*, 2888–2907. [CrossRef]
5. Vaughan, D.H.; Moses, H.L.; Blanton, J.C.; Baldwin, J.D. Design of Wind-Powered Cold Storage Facility Design of Wind-Powered Cold Storage Facility. October 1978. Available online: https://scholarsmine.mst.edu/cgi/viewcontent.cgi?article=1350&context=umr-mec (accessed on 13 March 2024).
6. Hameed, V.M.; Hussein, M.A. Studying the Performance of Refrigeration Units Powered by Solar Panel. *Iraqi J. Chem. Pet. Eng.* **2013**, *14*, 39–46. Available online: https://www.iasj.net (accessed on 13 March 2024).

7.   Yvon, R.; Nematchoua, M.K.; Chrysostome, R. Performance modelling of an electric vapor compression solar refrigeration system (SE-VCR) case for Madagascar. *Int. J. Front. Life Sci. Res.* **2021**, *1*, 028–051. [CrossRef]

8.   Roselli, C.; Sasso, M.; Tariello, F. A wind electric-driven combined heating, cooling, and electricity system for an office building in two Italian cities y. *Energies* **2020**, *13*, 895. [CrossRef]

9.   Fandi, O.M.; Dol, S.S.; Alavi, M. Review of Renewable Energy Applications and Feasibility of Tidal Energy in the United Arab Emirates. *Renew. Energy Res. Appl.* **2022**, *3*, 165–174. [CrossRef]

10.   Bernardino, M.; Rusu, L.; Soares, C.G. Evaluation of the wave energy resources in the Cape Verde Islands. *Renew. Energy* **2017**, *101*, 316–326. [CrossRef]

11.   Segurado, R.; Krajačić, G.; Duić, N.; Alves, L. Increasing the penetration of renewable energy resources in S. Vicente, Cape Verde. *Appl. Energy* **2011**, *88*, 466–472. [CrossRef]

12.   Shen, K.; Logozzo, P.; Sawant, M.; Yuan, B.; Bolis, N.; Shen, Y.; Li, B. Life-Cycle Assessment based Energy Consumption Analysis for Cold Food Storage Facilities. *Procedia CIRP* **2023**, *116*, 624–629. [CrossRef]

13.   Yenare, R.R.; Sonawane, C.R.; Sur, A.; Singh, B.; Panchal, H.; Kumar, A.; Sadasivuni, K.K.; Siddiqui, M.I.H.; Bhalerao, Y. A comprehensive review of portable cold storage: Technologies, applications, and future trends. *Alex. Eng. J.* **2024**, *94*, 23–33. [CrossRef]

14.   Wang, H.; Xie, B.; Li, C. Review on operation control of cold thermal energy storage in cooling systems. *Energy Built Environ.* 2024, *in press*. [CrossRef]

15.   Mahmood, R.A.; Ali, O.M.; Al-Janabi, A.; Al-Doori, G.; Noor, M.M. Review of Mechanical Vapour Compression Refrigeration System Part 2: Performance Challenge. *Int. J. Appl. Mech. Eng.* **2021**, *26*, 119–130. [CrossRef]

16.   Tebchirani, T.L.; Matos, R.S. Thermodynamic Analysis of a Refrigeration Cycle Using Regenerative Heat Exchanger-Suction/Liquid line. Available online: https://www.osti.gov/etdeweb/biblio/21564141 (accessed on 13 March 2024).

17.   Tashtoush, B.; Sahli, H.; Elakhdar, M.; Megdouli, K.; Nehdi, E. A new CO_2 refrigeration system with two-phase ejector and parallel compression for supermarkets. *Heliyon* **2024**, *10*, e27519. [CrossRef]

18.   Zhang, Z.; Wang, S.; Zhang, P.; Guan, Z.; Chang, L.; Wang, H. Effect of the refrigerant charge on transcritical CO_2 direct evaporation ice-making system. *Appl. Therm. Eng.* **2024**, *248*, 123283. [CrossRef]

19.   Fundamentals, A. *Wind Power Fundamentals*; Academic Press: Cambridge, MA, USA, 2017. [CrossRef]

20.   Kim, Y.-H.; Lim, H.-C. Effect of island topography and surface roughness on the estimation of annual energy production of offshore wind farms. *Renew. Energy* **2017**, *103*, 106–114. [CrossRef]

21.   Sathyajith, M. *Wind Energy Fundamentals, Resource Analysis and Economics*; Springer: Berlin, Germany, 2006.

22.   Brusca, S.; Capizzi, G.; Sciuto, G.L.; Susi, G. A new design methodology to predict wind farm energy production by means of a spiking neural network–based system. *Int. J. Numer. Model. Electron. Netw. Devices Fields* **2019**, *32*. [CrossRef]

23.   Ahmed, R.; Sreeram, V.; Mishra, Y.; Arif, M.D. A review and evaluation of the state-of-the-art in PV solar power forecasting: Techniques and optimization. *Renew. Sustain. Energy Rev.* **2020**, *124*, 109792. [CrossRef]

24.   Sepúlveda, F.J.; Montero, I.; Barrena, F.; Domínguez, M.A.; Miranda, M.T. Efficiency evaluation of photovoltaic systems with batteries considering different voltage levels. *J. Energy Storage* **2023**, *63*, 106971. [CrossRef]

25.   Mahjoob, A.; Ahmadi, P.; Afsaneh, H.; Vojdani, M.; Mortazavi, M. System sizing and transient simulation of a solar photovoltaic off-grid energy system in various climates with air heat pumps. *Sustain. Energy Technol. Assess.* **2022**, *54*, 102788. [CrossRef]

26.   Neill, S.P.; Haas, K.A.; Thiébot, J.; Yang, Z. A review of tidal energy—Resource, feedback, and environmental interactions. *J. Renew. Sustain. Energy* **2021**, *13*, 062702. [CrossRef]

27.   Nicholls-Lee, R.F.; Turnock, S.R. Tidal energy extraction: Renewable, sustainable and predictable. *Sci. Prog.* **2008**, *91*, 81–111. [CrossRef] [PubMed]

28.   Mehmood, N.; Liang, Z.; Khan, J. Harnessing Ocean Energy by Tidal Current Technologies. *Res. J. Appl. Sci. Eng. Technol.* **2012**, *4*, 3476–3487.

29.   Alaidroos, A. Transient Behavior Analysis of the Infiltration Heat Recovery of Exterior Building Walls. *Energies* **2023**, *16*, 7198. [CrossRef]

30.   Pereira, M.D.; de Oliveira, A.S. Analysis of the calculation of the thermal load of a cooling chamber of bovine carcasses with a capacity of 42 tons. *J. Eng. Exact. Sci.* **2020**, *6*, 0777–0782. [CrossRef]

31.   Hashim, H.M.; Sokolova, E.; Derevianko, O.; Solovev, D.B. Cooling Load Calculations. In *IOP Conference Series: Materials Science and Engineering*; Institute of Physics Publishing: Bristol, UK, 2018. [CrossRef]

32.   Bak, J.; Koo, J.; Yoon, S.; Lim, H. Thermal Draft Load Coefficient for Heating Load Differences Caused by Stack-Driven Infiltration by Floor in Multifamily High-Rise Buildings. *Energies* **2022**, *15*, 1386. [CrossRef]

33.   Ge, Y.T.; Tassou, S.A. Thermodynamic analysis of transcritical CO_2 booster refrigeration systems in supermarket. *Energy Convers. Manag.* **2011**, *52*, 1868–1875. [CrossRef]

34.   Escriva, E.J.S.; Acha, S.; Le Brun, N.; Francés, V.S.; Ojer, J.M.P.; Markides, C.N.; Shah, N. Modelling of a real CO_2 booster installation and evaluation of control strategies for heat recovery applications in supermarkets. *Int. J. Refrig.* **2019**, *107*, 288–300. [CrossRef]

35.   Maouris, G.; Escriva, E.J.S.; Acha, S.; Shah, N.; Markides, C.N. CO_2 refrigeration system heat recovery and thermal storage modelling for space heating provision in supermarkets: An integrated approach. *Appl. Energy* **2020**, *264*, 114722. [CrossRef]

36. Haque, A.; Khan, M.A.; Kurukuru, V.S. *Design and Control of Grid-Connected Photovoltaic System*; CRC Press: Boca Raton, FL, USA, 2023. [CrossRef]

37. Alvarez, D.L.; Al-Sumaiti, A.S.; Rivera, S.R. Estimation of an Optimal PV Panel Cleaning Strategy Based on Both Annual Radiation Profile and Module Degradation. *IEEE Access* **2020**, *8*, 63832–63839. [CrossRef]

38. Umar, N.H.; Bora, B.; Banerjee, C.; Umar, N.; Panwar, B.S. Comparison of different PV power simulation softwares: Case study on performance analysis of 1 MW grid-connected PV solar power plant. *Int. J. Eng. Sci. Invetion* **2018**, *7*, 11–24. Available online: https://www.ijesi.org (accessed on 13 March 2024).

39. Rodríguez, J.D.B.; Ramos-Paja, C.A.; Mejía, E.F. Modeling and parameter calculation of photovoltaic fields in irregular weather conditions. *Ingeniería* **2012**, *17*, 37–48. Available online: http://www.redalyc.org/articulo.oa?id=498850174006 (accessed on 13 March 2024).

40. PVGIS European Union. PVGIS-5 Geo-Temporal Irradiation Database. September 2023. Available online: https://joint-research-centre.ec.europa.eu/photovoltaic-geographical-information-system-pvgis_en (accessed on 4 November 2023).

41. Du, Z.; Gu, W. Aerodynamics analysis of wind power. In Proceedings of the WNWEC 2009–2009 World Non-Grid-Connected Wind Power and Energy Conference, Nanjing, China, 24–26 September 2009; pp. 235–237. [CrossRef]

42. Muchiri, K.; Kamau, J.N.; Wekesa, D.W.; Saoke, C.O.; Mutuku, J.N.; Gathua, J.K. Design and Optimization of a Wind Turbine for Rural Household Electrification in Machakos, Kenya. *J. Renew. Energy* **2022**, *2022*, 8297972. [CrossRef]

43. Biadgo, A.M.; Aynekulu, G. Aerodynamic design of horizontal axis wind turbine blades. *FME Trans.* **2017**, *45*, 647–660. [CrossRef]

44. Coelho, P. The Betz limit and the corresponding thermodynamic limit. *Wind. Eng.* **2022**, *47*, 491–496. [CrossRef]

45. Valery, L.O.; Sorensen, J.N. Refined Betz limit for rotors with a finite number of blades. *Wind. Energy Int. J. Prog. Appl. Wind. Power Convers. Technol.* **2008**, *11*, 415–426. [CrossRef]

46. Meteoblue. Meteorological Maps, Wind Gust. July 2023. Available online: https://www.meteoblue.com/pt/tempo/mapas/cidade-da-praia_cabo-verde_3374333#coords=4/14.93/-23.51&map=wind~hourly~auto~10%20m%20above%20gnd~none (accessed on 15 August 2023).

47. Meteoblue. Meteorological Maps, Ocean Currents. Lisbon. April 2023. Available online: https://www.meteoblue.com/pt/tempo/mapas/cidade-da-praia_cabo-verde_3374333#coords=4/14.93/-23.51&map=oceanCurrents~3hourly~auto~sfc~none (accessed on 4 August 2023).

48. Sengupta, A.; Gullo, P.; Dasgupta, M.S.; Khorshidi, V. Performance Analysis of an R744 Supermarket Refrigeration System Integrated with an Organic Rankine Cycle. *Energies* **2023**, *16*, 7478. [CrossRef]

49. Electra, S. Financial Statements 2022. Mindelo. 2023. Available online: https://www.bcv.cv/pt/Supervisao/Mercado%20de%20Capitais/Sistema/Emitentes/Presta%C3%A7%C3%A3o%20de%20Contas/Paginas/RCELECTRA.aspx (accessed on 1 November 2023).

50. Nugent, D.; Sovacool, B.K. Assessing the lifecycle greenhouse gas emissions from solar PV and wind energy: A critical meta-survey. *Energy Policy* **2014**, *65*, 229–244. [CrossRef]

51. Coutinho, G.L.; Vianna, J.N. Greenhouse Gas Emissions Avoided in Cape Verde: Estimation in a Scenario of Renewable Energy Sources Adoption in 2025. *LALCA Rev. Lat. Am. Em Avaliação Do Ciclo De Vida* **2020**, *4*, e45077. [CrossRef]

52. Imprensa Nacional de Cabo Verde SA. Official Gazette. Praia. December 2019. Available online: https://kiosk.incv.cv (accessed on 13 March 2024).